frontiers | Frontiers in Astronomy and Space Sciences

TYPE Original Research
PUBLISHED 08 August 2023
DOI 10.3389/fspas.2023.1232512

OPEN ACCESS

EDITED BY
Qianli Ma,
Boston University, United States

REVIEWED BY
Greg Cunningham,
Los Alamos National Laboratory (DOE), United States
Xin Tao,
University of Science and Technology of China, China

*CORRESPONDENCE
Solène Lejosne,
solene@berkeley.edu

RECEIVED 31 May 2023
ACCEPTED 13 July 2023
PUBLISHED 08 August 2023

CITATION
Lejosne S, Albert JM and Walton SD (2023), Drift phase resolved diffusive radiation belt model: 2. implementation in a case of random electric potential fluctuations.
Front. Astron. Space Sci. 10:1232512.
doi: 10.3389/fspas.2023.1232512

Drift phase resolved diffusive radiation belt model: 2. implementation in a case of random electric potential fluctuations

Solène Lejosne[1]*, Jay M. Albert[2] and Samuel D. Walton[1]

[1]Space Sciences Laboratory, University of California, Berkeley, CA, United States, [2]Air Force Research Laboratory, Kirtland AFB, Albuquerque, NM, United States

In the first part of this work, we highlighted a drift-diffusion equation capable of resolving the magnetic local time dimension when describing the effects of trapped particle transport on radiation belt intensity. Here, we implement these general considerations in a special case. Specifically, we determine the various transport and diffusion coefficients required to solve the drift-diffusion equation for equatorial electrons drifting in a dipole magnetic field in the presence of a specific model of time-varying electric fields. Random electric potential fluctuations, described as white noise, drive fluctuations of trapped particle drift motion. We also run a numerical experiment that consists of tracking trapped particles' drift motion. We use the results to illustrate the validity of the drift-diffusion equation by showing agreement in the solutions. Our findings depict how a structure initially localized in magnetic local time generates drift-periodic signatures that progressively dampen with time due to the combined effects of radial and azimuthal diffusions. In other words, we model the transition from a drift-dominated regime, to a diffusion-dominated regime. We also demonstrate that the drift-diffusion equation is equivalent to a standard radial diffusion equation once the distribution function is phase-mixed. The drift-diffusion equation will allow for radiation belt modeling with a better spatiotemporal resolution than radial diffusion models once realistic inputs, including localized transport and diffusion coefficients, are determined.

KEYWORDS

radiation belts, fokker-planck equation, adiabatic invariants, radial transport, radial diffusion, azimuthal diffusion, cross-terms, electric fields

1 Introduction

The effects of trapped particle spatial transport on radiation belt intensity are usually described by the radial diffusion paradigm. According to this model, in the absence of any other process besides spatial transport, the time evolution of radiation belt intensity is described by a one-dimensional diffusion equation:

$$\frac{\partial f(L^*,t)}{\partial t} = L^{*2}\frac{\partial}{\partial L^*}\left(\frac{D_{LL}}{L^{*2}}\frac{\partial f}{\partial L^*}\right) \quad (1)$$

where f is a distribution function proportional to phase space density, L^* is inversely proportional to the third adiabatic invariant, and $D_{LL} = \left\langle \left(\Delta L^*\right)^2 \right\rangle / 2$ is the radial diffusion coefficient (Roederer, 1970). Since all the quantities involved in Eq. 1 are *drift-averaged*, i.e., averaged over all three gyration, bounce and drift phases, there is no information on trapped particle drift phase—or equivalently, on the magnetic local time (MLT) dimension. In a companion paper (Lejosne and Albert, 2023), we discussed the limitations associated with the inability to resolve the drift phase. We also proposed a theoretical solution to address this difficulty. Namely, we highlighted a two-dimensional drift-diffusion equation to describe trapped particle transport effects on radiation belt intensity (Birmingham et al., 1967). According to this model, in the absence of any other process besides transport, radiation belt intensity varies such that:

$$\frac{\partial F(\mathbb{L},\varphi,t)}{\partial t} = -[\dot{\mathbb{L}}]\frac{\partial F}{\partial \mathbb{L}} - [\dot{\varphi}]\frac{\partial F}{\partial \varphi} + \mathbb{L}^2 \frac{\partial}{\partial \mathbb{L}}\left(\frac{D_{\mathbb{L}\mathbb{L}}}{\mathbb{L}^2}\frac{\partial F}{\partial \mathbb{L}}\right) + \mathbb{L}^2 \frac{\partial}{\partial \mathbb{L}}\left(\frac{D_{\mathbb{L}\varphi}}{\mathbb{L}^2}\frac{\partial F}{\partial \varphi}\right) + \frac{\partial}{\partial \varphi}\left(D_{\varphi\mathbb{L}}\frac{\partial F}{\partial \mathbb{L}}\right) + \frac{\partial}{\partial \varphi}\left(D_{\varphi\varphi}\frac{\partial F}{\partial \varphi}\right) \tag{2}$$

where F is a distribution function proportional to the number of particles per unit of surface, $d\mathbb{L}d\varphi$, φ is the azimuthal location (i.e., MLT, in radians), and the "double-struck L" (or "L-Euler") coordinate is: $\mathbb{L} = 1/\sin^2\theta_E$, with θ_E the magnetic colatitude of the intersection between the Earth's surface and the footpoint of the field line passing through the location considered. The parameters $D_{\mathbb{L}\mathbb{L}}$, $D_{\varphi\varphi}$, $D_{\mathbb{L}\varphi}$ and $D_{\varphi\mathbb{L}}$ are the MLT-dependent diffusion coefficients, and the parameters $[\dot{\mathbb{L}}]$ and $[\dot{\varphi}]$, also MLT-dependent, are the mean time rates of change of $\mathbb{L}$ and φ. All the quantities involved in Eq. 2 are *bounce-averaged* quantities that depend on MLT. In particular, the coordinate double-struck L, $\mathbb{L}$, corresponds to the normalized equatorial radius of the field line on which trapped particles would bounce if all non-dipolar contributions to the magnetic field were turned off on a timescale comparable to a few bounce periods. There are various benefits of using L-Euler as a coordinate for radial transport over L-McIlwain or L-Roederer. From the theoretical standpoint, the set of coordinates $(\mathbb{L},\varphi)$ is proportional to a set of canonical variables, which allows for a reduction of the general two-dimensional Fokker-Planck equation into a drift-diffusion equation (Eq. 2) (Lejosne and Albert, 2023). In addition, computing the L-Euler, $\mathbb{L}$, is much less expensive than computing the L-Roederer, L^*, coordinate: The former only requires local field line tracing, while the latter requires computing the magnetic flux through the instantaneous drift shell. The set of coordinates $(\mathbb{L},\varphi)$ can also be used to parameterize both trapped and quasi-trapped populations (since the definition of L-Euler, $\mathbb{L}$, only requires a closed local field line). On the other hand, the L^* parameter requires a closed instantaneous drift shell, meaning that it can only parameterize trapped populations. Thus, the L-Euler, $\mathbb{L}$, is an appropriate coordinate for modeling the trapping and de-trapping of energetic particles at transition regions (e.g., close to the magnetopause, or at low L regions, below the inner radiation belt).

In the following, we specify the field and particle characteristics assumed to compute the transport and diffusion coefficients introduced in Eq. 2 in a special case. For the sake of simplicity, we focus on the magnetic equator and assume dipolar magnetic field lines thereafter. In this context, $\mathbb{L} = L = r/R_E$, where r is the equatorial radius and $R_E = 6,370\,\text{km}$ is one Earth's equatorial radius.

2 Theoretical setup

The objective of this section is to show how to determine the localized transport ($[\dot{\mathbb{L}}]$ and $[\dot{\varphi}]$) and diffusion ($D_{\mathbb{L}\mathbb{L}}$, $D_{\varphi\varphi}$, $D_{\mathbb{L}\varphi}$ and $D_{\varphi\mathbb{L}}$) coefficients in the simple case of equatorially mirroring particles trapped in a magnetic dipole field with a drift motion perturbed by a special case of random electric potential fluctuations. The characteristics of the fields are provided in Section 2.1, and their effects on the drift motion of trapped particles are detailed in Section 2.2.

2.1 Fields

We assume a magnetic dipole field, **B,** and an electric potential, V, whose random time variations lead to small perturbations of trapped particle drift motion. The dipole field at the magnetic equator in spherical coordinates (r,θ,φ) is:

$$\mathbf{B} = \begin{pmatrix} 0 \\ -\frac{B_E R_E^3}{r^3} \\ 0 \end{pmatrix} \tag{3}$$

where $B_E = 30,000\,\text{nT}$ is the magnetic equatorial field at the Earth's surface. We model the total electric potential, V, as the sum of a well-determined corotation potential, and some *ad hoc* fluctuations proportional to a random variable, w:

$$V = -\frac{C}{r} + w(t) r\cos\varphi \tag{4}$$

where $C = \Omega_E B_E R_E^3$ is a constant, with $\Omega_E = 2\pi/86400\,\text{s} \cong 7.3\,e^{-5}\,\text{s}^{-1}$ the angular velocity of the Earth's rotation, so $-C/r$ is the corotation potential. The electric field, $\mathbf{E} = -\nabla V$, at the magnetic equator is:

$$\mathbf{E} = \begin{pmatrix} -\frac{C}{r^2} - w(t)\cos\varphi \\ 0 \\ w(t)\sin\varphi \end{pmatrix} \tag{5}$$

Characteristics of the electric fluctuation: The electric fluctuation, w(t) (in V/m), is assumed to be not well known. This lack of determination in field variations is what drives the need for a stochastic model, rather than a deterministic one. We view the electric fluctuation, w(t), as a sequence of possible outcomes by a random variable. In this first implementation, we favor practicality over realism to characterize the properties of the variable. Specifically, we assume that the variable, w, is a white noise. We describe it as a piecewise constant function: the value stays constant for a set amount of time, T (in seconds), and it updates instantaneously and unpredictably at the end of every time interval. We choose the size of the time interval, T, such that the time variations of the electric fluctuation, w(t), result in the variation of the third adiabatic invariant, while conserving the first two invariants of the population considered. In other words, we

require that $\tau_B \ll T \ll \tau_D$, where τ_B and τ_D are the bounce and drift periods, respectively. This assumption differs from the drift resonance condition, where $T \sim \tau_D$.

The standard deviation of the white noise, W, is a parameter that we set arbitrarily. The mean value of the white noise, [w], is theoretically 0, by definition. Yet, when considering a finite sequence of values for w(t), the ensemble average is not necessarily 0 in practice. Thereafter, we consider that the average value, [w], remains small enough that: $[w]^2 \ll \Omega T W^2$, where $\Omega/2\pi$ is the unperturbed drift frequency. This assumption is verified in our numerical experiment, and it simplifies mathematical derivations.

2.2 Trapped particles

2.2.1 Computation of the localized transport and diffusion coefficients

The objective of this Section is to determine $D_{\mathbb{L}\mathbb{L}}$, $D_{\varphi\varphi}$, $D_{\mathbb{L}\varphi}$ and $D_{\varphi\mathbb{L}}$, the diffusion coefficients, and $[\dot{\mathbb{L}}]$ and $[\dot{\varphi}]$, the transport coefficients, defined as the mean time rates of change of the radial and azimuthal locations, respectively. This is done for a population of equatorially trapped particles drifting in the fields described in Section 2.1. Generally speaking, a diffusion coefficient for a set of variables, X and Y, is:

$$D_{XY} = \frac{\langle \Delta X \Delta Y \rangle}{2} \tag{6}$$

where $\langle \Delta X \Delta Y \rangle = [\Delta X \Delta Y]/\Delta t$ is the rate of change of the expected value for the product of the time variations of X and Y during a time interval, Δt:

$$[\Delta X \Delta Y] = [(X(t+\Delta t) - X(t))(Y(t+\Delta t) - Y(t))] \tag{7}$$

In our case, the time interval, Δt, is long with respect to the bounce period, but very small in comparison with the drift period, $\tau_B \ll \Delta t \ll \tau_D$. Thus, we need to compute the time variations for the radial and azimuthal locations of the trapped particles, Δr and $\Delta\varphi$, respectively, to determine the diffusion coefficients.

The equations for the drift motion of equatorial particles trapped in the fields described in Section 2.1 are:

$$\begin{pmatrix} \dot{r} \\ 0 \\ \dot{\varphi} \end{pmatrix} = \begin{pmatrix} \frac{r^3}{B_E R_E^3} w(t) \sin\varphi \\ 0 \\ -\frac{3M}{\gamma q r^2} + \Omega_E + \frac{r^2}{B_E R_E^3} w(t) \cos\varphi \end{pmatrix} \tag{8}$$

where M is the first adiabatic invariant, q is the electric charge of the particle and γ is the Lorentz factor. Given that $\dot{\mathbb{L}} = \dot{r}/R_E$ at the magnetic equator of a dipole field, the transport coefficients are:

$$\begin{cases} [\dot{\mathbb{L}}] = \frac{\mathbb{L}^3 [w]}{B_E R_E} \sin\varphi \\ [\dot{\varphi}] = \Omega + \frac{\mathbb{L}^2 [w]}{B_E R_E} \cos\varphi \end{cases} \tag{9}$$

where $\Omega = -3M/\gamma q R_E^2 \mathbb{L}^2 + \Omega_E$ is the unperturbed angular drift velocity. In the presence of an ideal white noise signal ($[w] = 0$) the transport coefficients become $[\dot{\mathbb{L}}] = 0$ and $[\dot{\varphi}] = \Omega$.

Using Eq. 8, the general expressions for the total variations in radial and azimuthal locations after a time interval Δt are, respectively:

$$\begin{cases} \Delta r = \frac{1}{B_E R_E^3} \int_t^{t+\Delta t} r^3(u) w(u) \sin\varphi(u) du \\ \Delta\varphi = -\frac{3M}{q} \int_t^{t+\Delta t} \frac{1}{\gamma(u) r^2(u)} du + \Omega_E \Delta t + \frac{1}{B_E R_E^3} \int_t^{t+\Delta t} r^2(u) w(u) \cos\varphi(u) du \end{cases} \tag{10}$$

We consider a time interval, Δt, very small in comparison with the drift period ($\Delta t \ll \tau_D$), but long enough to have many small fluctuations during Δt ($T \ll \Delta t$). We also assume small radial displacements ($\Delta r/r \ll 1$). As detailed in the **Appendix**, it results that:

$$\begin{cases} \langle (\Delta r)^2 \rangle = \frac{r^6 W^2 T}{B_E^2 R_E^6} \sin^2\varphi \\ \langle (\Delta\varphi)^2 \rangle = \frac{r^4 W^2 T}{B_E^2 R_E^6} \cos^2\varphi \\ \langle \Delta r \Delta\varphi \rangle = \langle \Delta\varphi \Delta r \rangle = \frac{r^5 W^2 T}{B_E^2 R_E^6} \sin\varphi \cos\varphi \end{cases} \tag{11}$$

With the definition provided Eq. 6, the MLT-localized diffusion coefficients are:

$$\begin{cases} D_{\mathbb{L}\mathbb{L}} = \frac{\mathbb{L}^6 W^2 T}{2 B_E^2 R_E^2} \sin^2\varphi \\ D_{\varphi\varphi} = \frac{\mathbb{L}^4 W^2 T}{2 B_E^2 R_E^2} \cos^2\varphi \\ D_{\mathbb{L}\varphi} = D_{\varphi\mathbb{L}} = \frac{\mathbb{L}^5 W^2 T}{2 B_E^2 R_E^2} \sin\varphi \cos\varphi \end{cases} \tag{12}$$

We note that the diffusion coefficients provided in Eq. 12 are functions of magnetic local time, φ. This is in contrast with the standard radial diffusion coefficient, independent of magnetic local time by definition, which involves drift-phase averaging (e.g., Lejosne and Kollmann, 2020). The relationship between these coefficients and the standard radial diffusion framework is further discussed in Section 3.1.

The diffusion coefficients provided in Eq. 12 are also proportional to W^2T, the product of the variance of the random signal, w, and a time, T, that is similar to an autocorrelation time. This finding is consistent with theoretical expectations: the higher the variance, the stronger the perturbation, the higher the diffusion. We also expect electric field perturbations that stay correlated for a longer time interval to be more efficient in perturbing drift motion. On the other hand, the coefficients are independent of the energy of the trapped population considered, provided that the updating time, T, remains very small in comparison with the drift period (see also the discussion in **Appendix**). The coefficients are also independent of the charge of the population. These findings would need to be reassessed in the presence of more realistic field perturbations.

2.2.2 Contextualization using Hamiltonian equations

We expect a relationship between the first and second moments characterizing transport. Indeed, assuming small variations over the course of a couple of bounce periods,we have shown in the first part

of this work (Lejosne and Albert, 2023) that:

$$\begin{cases} -\langle\Delta\alpha\rangle + \frac{1}{2}\frac{\partial\langle(\Delta\alpha)^2\rangle}{\partial\alpha} + \frac{1}{2}\frac{\partial\langle\Delta\alpha\Delta\beta\rangle}{\partial\beta} = -[\dot{\alpha}] \\ -\langle\Delta\beta\rangle + \frac{1}{2}\frac{\partial\langle(\Delta\beta)^2\rangle}{\partial\beta} + \frac{1}{2}\frac{\partial\langle\Delta\beta\Delta\alpha\rangle}{\partial\alpha} = -[\dot{\beta}] \end{cases} \tag{13}$$

where (α,β) are the Euler potentials. In a dipole field at the magnetic equator, given that $\alpha \propto 1/r$, and $\beta = \varphi$, this set of equations is equivalent to:

$$\begin{cases} -\langle\Delta r\rangle + \frac{r^2}{2}\frac{\partial}{\partial r}\left(\frac{\langle(\Delta r)^2\rangle}{r^2}\right) + \frac{1}{2}\frac{\partial}{\partial\varphi}\left(\langle\Delta r\Delta\varphi\rangle\right) = -[\dot{r}] \\ -\langle\Delta\varphi\rangle + \frac{1}{2}\frac{\partial\langle(\Delta\varphi)^2\rangle}{\partial\varphi} + \frac{r^2}{2}\frac{\partial}{\partial r}\left(\frac{\langle\Delta\varphi\Delta r\rangle}{r^2}\right) = -[\dot{\varphi}] \end{cases} \tag{14}$$

A second-order Taylor expansion of Eq. 10 yields

$$\begin{cases} \langle\Delta r\rangle = \frac{r^3[\mathrm{w}]}{\mathrm{B_E R_E^3}}\sin\varphi + \frac{\mathrm{r^5 W^2 T}}{\mathrm{B_E^2 R_E^6}}\left(\frac{1}{2} + \sin^2\varphi\right) \\ \langle\Delta\varphi\rangle = \Omega + \frac{r^2[\mathrm{w}]}{\mathrm{B_E R_E^3}}\cos\varphi + \frac{\mathrm{r^4}W^2T}{2\mathrm{B_E^2 R_E^6}}\sin\varphi\cos\varphi \end{cases} \tag{15}$$

Leveraging Eqs 9, 11 and 15, it is straightforward to verify Eq. 14. A notable consequence of this result is that:

$$\langle\Delta r\rangle \neq \frac{r^2}{2}\frac{\partial}{\partial r}\left(\frac{\langle(\Delta r)^2\rangle}{r^2}\right) \tag{16}$$

when the drift phase is resolved. In other words, the commonly assumed relationship between the first and second moments of radial transport, $\langle\Delta r\rangle$ and $\langle(\Delta r)^2\rangle$ (e.g., Fälthammar, 1968, their Eq. 3), is verified only on average over all magnetic local times.

3 On the drift-diffusion equation

3.1 Equivalence with a radial diffusion equation in the case of an azimuthally symmetric distribution function

We leverage the coefficients computed in Section 2.2 to demonstrate that Eq. 2 is like a radial diffusion equation (Eq. 1) when the distribution function is independent of MLT, i.e., when $\partial F/\partial\varphi = 0$. Eq. 2 becomes:

$$\frac{\partial F}{\partial t} = -[\dot{\mathbb{L}}]\frac{\partial F}{\partial\mathbb{L}} + \mathbb{L}^2\frac{\partial}{\partial\mathbb{L}}\left(\frac{D_{\mathbb{L}\mathbb{L}}}{\mathbb{L}^2}\frac{\partial F}{\partial\mathbb{L}}\right) + \frac{\partial}{\partial\varphi}\left(D_{\varphi\mathbb{L}}\right)\frac{\partial F}{\partial\mathbb{L}} \tag{17}$$

when $\partial F/\partial\varphi = 0$. This is also:

$$\frac{\partial F}{\partial t} = -[\dot{\mathbb{L}}]\frac{\partial F}{\partial\mathbb{L}} + D_{\mathbb{L}\mathbb{L}}\frac{\partial^2 F}{\partial\mathbb{L}^2} + \left(\mathbb{L}^2\frac{\partial}{\partial\mathbb{L}}\left(\frac{D_{\mathbb{L}\mathbb{L}}}{\mathbb{L}^2}\right) + \frac{\partial}{\partial\varphi}\left(D_{\varphi\mathbb{L}}\right)\right)\frac{\partial F}{\partial\mathbb{L}} \tag{18}$$

Leveraging Equations 9, 12 yields:

$$\begin{aligned}\frac{\partial F}{\partial t} = &-\frac{\mathbb{L}^3[\mathrm{w}]}{\mathrm{B_E R_E}}\sin\varphi\frac{\partial F}{\partial\mathbb{L}} + \frac{\mathbb{L}^6 W^2 T}{2\mathrm{B_E^2 R_E^2}}\sin^2\varphi\frac{\partial^2 F}{\partial\mathbb{L}^2} \\ &+ \left(\frac{\mathbb{L}^5\mathrm{W^2T}}{2\mathrm{B_E^2 R_E^2}}\left(1 + 2\sin^2\varphi\right)\right)\frac{\partial F}{\partial\mathbb{L}}\end{aligned} \tag{19}$$

Averaging over all MLT-phases, we have that:

$$\frac{\partial F}{\partial t} = \frac{\mathbb{L}^6 W^2 T}{4\mathrm{B_E^2 R_E^2}}\frac{\partial^2 F}{\partial\mathbb{L}^2} + \frac{\mathbb{L}^5\mathrm{W^2T}}{\mathrm{B_E^2 R_E^2}}\frac{\partial F}{\partial\mathbb{L}} \tag{20}$$

Introducing the drift-averaged diffusion coefficient, D_{LL}, as:

$$D_{LL} = \frac{\mathbb{L}^6 W^2 T}{4\mathrm{B_E^2 R_E^2}} \tag{21}$$

Equation 20 also becomes:

$$\frac{\partial F}{\partial t} = L^2\frac{\partial}{\partial L}\left(\frac{D_{LL}}{L^2}\frac{\partial F}{\partial L}\right) \tag{22}$$

We emphasize that $\mathbb{L} = L = r/R_E$ in this demonstration, since we assume a dipole magnetic field. Given that the phase-averaged distribution function, f, is proportional to the bounce-averaged distribution function, F, by a physical constant when F is independent on MLT, Eq. 22 can be rewritten as:

$$\frac{\partial f}{\partial t} = L^2\frac{\partial}{\partial L}\left(\frac{D_{LL}}{L^2}\frac{\partial f}{\partial L}\right) \tag{23}$$

Thus, we have shown how the drift-diffusion Eq. 2 relates to the standard radial diffusion Eq. 1 when the distribution function is phase-mixed (i.e., independent of MLT). We have also shown that the corresponding radial diffusion coefficient, D_{LL}, is the MLT-average of the localized radial diffusion coefficient, $D_{\mathbb{L}\mathbb{L}}$. The expression for D_{LL} provided Eq. 21 is the same as the one that would be obtained by following standard procedures to compute radial diffusion coefficients (e.g., Schulz and Lanzerotti, 1974, their section III.3).

3.2 Change of variables to remove the cross terms

The drift-diffusion equation (Eq. 2) contains cross-terms ($\mathrm{D\mathbb{L}\varphi} = \mathrm{D\varphi\mathbb{L}} \neq 0$), which poses numerical challenges to guarantee positivity of the solution (Tao et al., 2008; 2009; 2016). Albert and Young (2005) and Albert (2018) discussed changes of coordinates to address this difficulty. In the present situation, the determinant of the 2×2 diffusion matrix is 0:

$$D_{\mathbb{L}\mathbb{L}}D_{\varphi\varphi} - D_{\mathbb{L}\varphi}^2 = 0 \tag{24}$$

This means that 0 is an eigenvalue of the diffusion matrix, and there exists a system of coordinates in which the diffusive part of the drift-diffusion equation is one-dimensional. We introduce a new set of variables:

$$\begin{cases} x = \mathbb{L}\cos\varphi \\ y = \mathbb{L}\sin\varphi \end{cases} \tag{25}$$

which corresponds to a conversion from polar to Cartesian coordinates. In this coordinate system, with the values of the diffusion coefficients provided Eq. 12, Eq. 2 becomes:

$$\frac{\partial F}{\partial t} = -[\dot{x}]\frac{\partial F}{\partial x} - [\dot{y}]\frac{\partial F}{\partial y} + \left(x^2 + y^2\right)^{\frac{3}{2}}\frac{\partial}{\partial y}\left(\frac{D_{yy}}{\left(x^2 + y^2\right)^{\frac{3}{2}}}\frac{\partial F}{\partial y}\right) \tag{26}$$

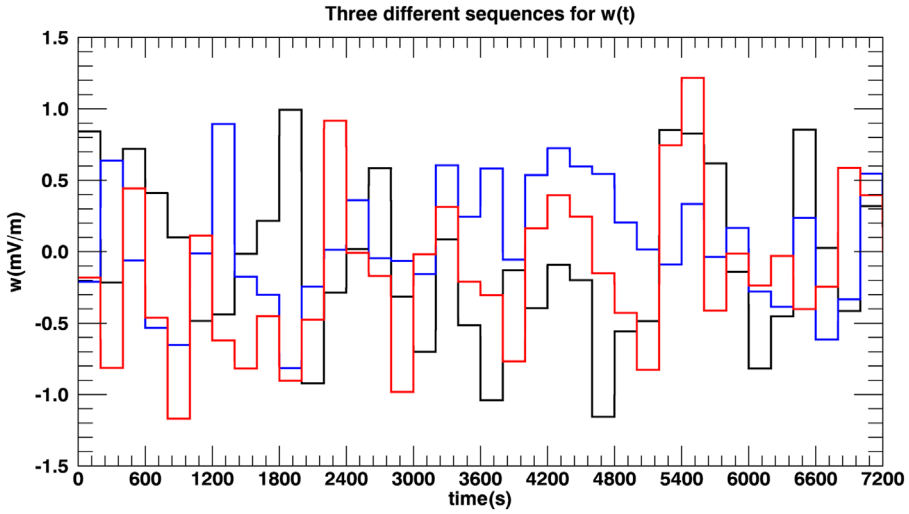

FIGURE 1
Three different sequences of randomly generated outcomes for the white noise signal, *w* (t), are represented in black, blue and red over a 2-h time interval. The signal is updated every T = 200 s. The expected (i.e., average) value is 0 mV/m, and the standard deviation is set to 0.5 *mV/m*.

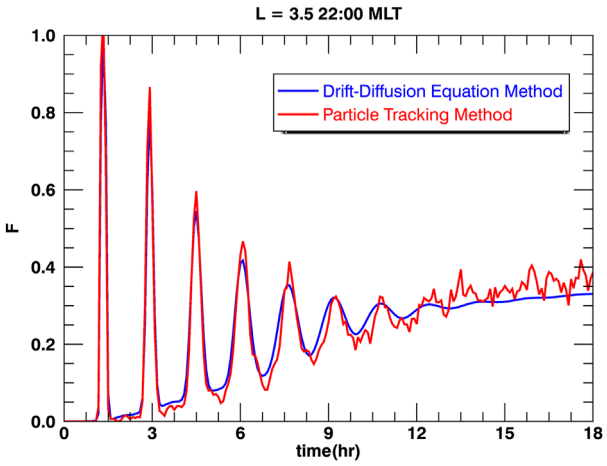

FIGURE 2
Time evolution of the distribution function centered at L = 3.5 and 22:00 MLT. The magnitude of the flux oscillation characteristic of trapped particle injections decreases with time until it vanishes after a time characteristic of phase mixing. This figure compares numerical results from (in red) a test particle simulation and (in blue) the solution of the drift-diffusion equation. It illustrates the transition from a drift-dominated regime (with the presence of drift periodic oscillations in the distribution function) to a diffusion-dominated regime (characterized by a slow and steady variation of the distribution function).

with

$$D_{yy} = \frac{W^2 T}{2B_E^2 R_E^2}(x^2 + y^2)^3 \tag{27}$$

Looking back at the drift motion equations (Eq. 8), we notice that the perturbation of the drift velocity is indeed along the *y*-direction: The velocity perturbation is along $\sin\varphi \boldsymbol{e_r} + \cos\varphi \boldsymbol{e_\varphi} = \boldsymbol{e_y}$, where $\boldsymbol{e_y}$ and $\boldsymbol{e_r}, \boldsymbol{e_\varphi}$ are unit vectors associated with the Cartesian and polar frames of reference.

In the following, we assume [w] = 0 for the sake of simplicity. This means that $[\dot{\mathbb{L}}] = 0$ and $[\dot{\varphi}] = \Omega$. As a result, Eq. 26 is also:

$$\frac{\partial F}{\partial t} = -\Omega \frac{\partial F}{\partial \varphi} + \mathbb{L}^3 \frac{\partial}{\partial y}\left(\frac{D_{yy}}{\mathbb{L}^3}\frac{\partial F}{\partial y}\right) \tag{28}$$

This latest equation is the one used for numerical implementation, as discussed in Section 4.

4 Numerical simulations

4.1 Numerical setups and methods

Parameters: Since this work assumes electric potential fluctuations in a time-stationary dipole field, we focus on a region where this is most likely to happen, namely, the inner belt and slot region (below L = 4). We consider populations that have been associated with drift period structures in this region, i.e., electrons in the tens to hundreds of keV energy range (e.g., Ukhorskiy et al., 2014). Specifically, we focus on equatorial electrons with kinetic energy of 200 keV at $L = 3$. These electrons have a first adiabatic invariant of M = 21.5 MeV/G, and a second adiabatic invariant of $J = 0$. The standard deviation of the white noise, W, is a parameter that we set to a plausible value of about 0.5 mV/m ($W^2 = 2.5 \times 10^{-7} V^2/m^2$). We set the updating time (i.e., the duration between changes in value) for the sequence of outcomes w(t) to be $T = 200s$. At L = 3, the bounce and drift periods of the electrons considered are $\tau_B \sim 0.4s$ and $\tau_D \sim 1.5hr$, so the ordering, $\tau_B \ll T \ll \tau_D$, is verified. With this set of parameters, the coefficient of proportionality for the diffusion coefficients is $W^2 T/2B_E^2 R_E^2 = 6.8 \times 10^{-10} s^{-1} = 5.9 \times 10^{-5} day^{-1}$. Therefore, given Eq. 21, the drift-averaged diffusion coefficient D_{LL} is set to $D_{LL} \sim 3.0 \times 10^{-5} L^6 day^{-1}$ ($2.2 \times 10^{-2} day^{-1}$ at L =

3 for instance). This order of magnitude is consistent with previous estimates for radial diffusion in the inner belt and slot region (e.g., Selesnick, 2012; O'Brien et al., 2016, their Figure 4).

Method for particle tracking: We solve Eq. 8 to determine trapped particle drift motion. We launch particles in many different sequences of outcomes for w (t). We use the RANDOMN function from IDL, which returns pseudorandom numbers from a Gaussian distribution to generate an original time sequence of outcomes. Every different sequence is created by randomly reordering (permuting) the vector indices of the original sequence of outcomes. To create a permutation of the vector indices, we use the RANDOMU function from IDL, which returns an array of uniformly distributed random numbers. An illustration of the approach is provided in Figure 1. It represents three different permutations for the sequence of outcomes for w(t), over a time intervals of 2 h. For the numerical experiment, we perform 200 different permutations. We track more than 10,000 particle drift trajectories for 18 h every time, recording their locations every 5 min. The particle initial locations are distributed homogeneously, following the initial condition described hereafter.

Initial condition: To solve numerically Eq. 28, we consider a simple initial condition, assuming that:

- Particles are present homogeneously at all MLTs at $3.8\,R_E$ and above (up to 7 R_E).
- Particles are also present homogeneously in an area mimicking a localized injection, extending from $r = 2.5\,R_E$ to $r = 3.8\,R_E$, and initially centered around 00:00 MLT (from 22:15 to 01:45).

The distribution function, F, is chosen to be initially constant and normalized (= 1) at all locations where particles are present. It is set to zero otherwise.

Method for numerical simulation: To solve numerically Eq. 28, we use an operator splitting method. At each time step, we first solve the transport part of the equation, using the method of characteristics. We then use the updated function to solve the diffusive part of the equation, using an explicit scheme for the sake of simplicity. We record the value of the distribution function, F, every 5 min over a 24-h interval.

4.2 Results

4.2.1 Comparison between the results of the test particle experiments and the solution of the drift-diffusion equation

We compare: a) the outputs of the particle tracking experiment with b) the solution of Eq. 28. First, we focus on one location (L = 3.5 ± 0.05 and 22:00 MLT ± 00:15): We record the time evolution of the distribution functions derived from the drift-diffusion equation and from the particle tracking experiment. The results, presented in Figure 2**,** highlight the consistency of the two approaches. The location is initially out of the artificial injection region thus $F(t = 0) = 0$. As the particles drift eastwards starting from the midnight region, no particles are visible for a moment. Then, they briefly drift through the location, creating a transient peak in the distribution function, and so on. Figure 2 shows how the distribution function oscillates at the trapped particles'

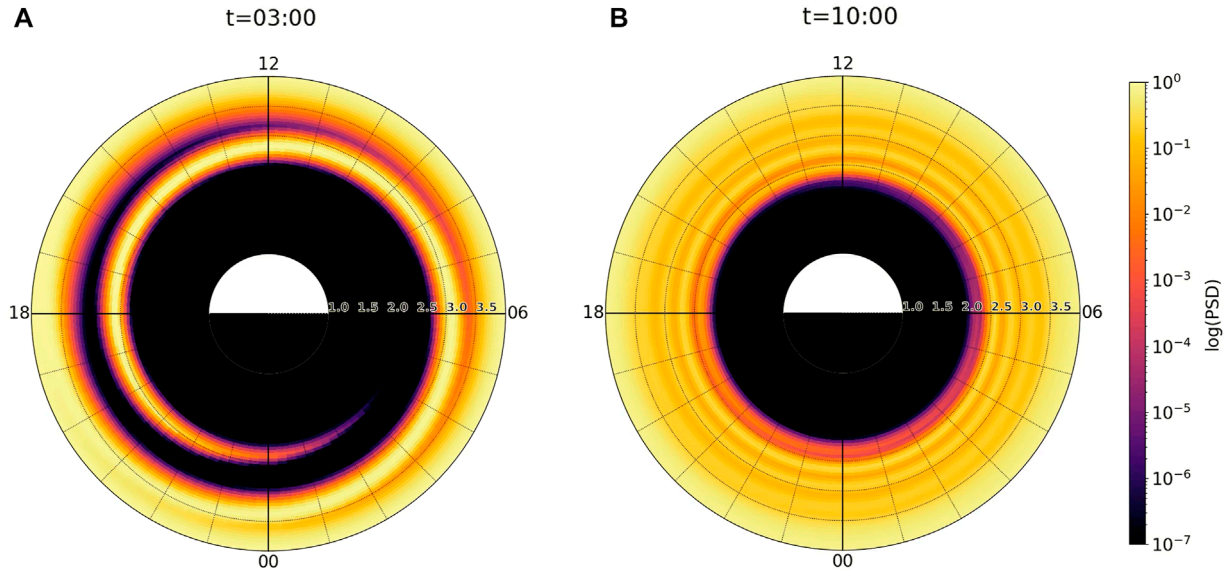

FIGURE 3
Time evolution of a distribution function (initially centered around 00:00 MLT for $2.5\,R_E < r < 3.8\,R_E$, and constant at all MLTs for $r \geq 3.8\,R_E$) **(A)** At t = 3:00 h, the MLT-dependent structure is visible. It creates a spiral around the Earth due to the L-dependence of the drift frequency. As a result, the distribution function is strongly dependent on MLT for r between ~ $2.5\,R_E$ and $3.8\,R_E$ **(B)** At t = 10:00 h, the MLT-dependent structure has disappeared: The distribution function is barely dependent on MLT. The effect of transport on radiation belt intensity is now more consistent with the radial diffusion paradigm.

unperturbed drift frequency. With time, the magnitude of the peak decreases, and the width of the peak increases: This is due to the combined effects of radial and azimuthal diffusions. In parallel, new particles transported radially from L ≥ 3.8 fill the region: The drift-averaged minimum of the distribution function increases with time. After some time, the drift-periodic signature disappears and the regime is purely diffusive. In other words: In this numerical experiment, the radial diffusion equation represents a valid description of the system after ~15 h at L = 3.5 (or about 9 drift periods for the population considered). For shorter times, it is necessary to use the drift-diffusion equation to represent the time evolution of drift echoes. In general, we expect the magnitude of the typical phase-mixing time scale to be a function of: (a) the initial condition for the distribution function (the more MLT-localized the inhomogeneity, the longer it will take to cover all MLT sectors), (b) the magnitude of the diffusion coefficients (the higher the coefficient, the most efficient at smoothing MLT-dependent fluctuations, thus the shorter the characteristic time for phase mixing) and (c) the drift frequency (the higher the drift frequency, the shorter the characteristic time for phase mixing).

4.2.2 Visualization of the solution of the drift-diffusion equation

A 2D video of the simulation run for the solution of the drift-diffusion equation over a 24 h interval is provided in Supplementary Material. Two screenshots (at t = 3:00 h and t = 10:00 h) are provided in Figure 3.

From the video, it is clear that the effect of the azimuthal drift on radiation belt intensity is at first more striking than the effects of radial and azimuthal diffusion. That said, drift alone would only lead to trajectories wrapping around, meaning that the distribution function would only become more structured. Radial and azimuthal diffusions act to smooth out the MLT-dependent structure, dampening it until it disappears and the distribution becomes independent of MLT. This *phase-mixing* process is consistent with observations. It allows for the transition from a drift-dominated regime to a diffusion-dominated regime.

5 Conclusion

We have shown how the drift-diffusion equation is capable of modeling phase mixing, allowing for a transition from drift-resolved structures (e.g., drift-periodic fluctuations associated with MLT-localized sources or losses) to the standard radial diffusion framework. We illustrated our case using simple assumptions, focusing on the magnetic equator of a dipole field and modeling electric potential fluctuations by a white noise. A next step of physical importance is to model the effect of the thermospheric wind driven electric field fluctuations on radiation belt dynamics. Indeed, electric potential fluctuations are present in the inner belt. They are viewed as the primary driver of radial diffusion in this region (e.g., O'Brien et al., 2016). In particular, electric fluctuations associated with quiet time wind dynamo have significant day-to-day variability, even during geomagnetically quiet periods (e.g., Fejer, 1993). Thermospheric wind driven electric fields are also known to shape the inner belt drift shells (Lejosne et al., 2021). Future work should consist of determining a more realistic form for the electric perturbation using information on thermospheric wind driven electric field fluctuations. Going back to the general expression of the drift-diffusion equation, future work should also consist of determining the various transport and diffusion coefficients in the presence of a time varying magnetic field. Once realistic inputs, including localized transport and diffusion coefficients, are determined, the drift-diffusion equation will enable operational radiation belt modeling with a better spatiotemporal resolution than current radial diffusion models.

Data availability statement

The raw data supporting the conclusion of this article will be made available by the authors, without undue reservation.

Author contributions

We describe contributions to the paper using the CRediT (Contributor Roles Taxonomy) categories (Brand et al., 2015). Conceptualization, Writing—Original Draft: SL and JA Writing—Review and Editing: All authors. Visualization: SL and SW. All authors contributed to the article and approved the submitted version.

Funding

SL work was performed under NASA Grant Awards 80NSSC18K1223 and 80NSSC20K1351. SW work was performed under NASA Grant Award 80NSSC20K1351. JA was supported by NASA grant 80NSSC20K1270, AFOSR grant 22RVCOR002, and the Space Vehicles Directorate of the Air Force Research Laboratory.

Conflict of interest

The authors declare that the research was conducted in the absence of any commercial or financial relationships that could be construed as a potential conflict of interest.

Publisher's note

Author disclaimer

The views expressed are those of the authors and do not reflect the official guidance or position of the United States Government, the Department of Defense or of the United States Air Force. The appearance of external hyperlinks does not constitute endorsement by the United States Department of Defense (DoD) of the linked websites, or the information, products, or services contained therein. The DoD does not exercise any editorial, security, or other control over the information you may find at these locations.

Supplementary material

The Supplementary Material for this article can be found online at: https://www.frontiersin.org/articles/10.3389/fspas.2023.1232512/abstract#supplementary-material

References

Albert, J. M. (2018). Diagonalization of diffusion equations in two and three dimensions. *J. Atmos. Solar-Terrestrial Phys.* 177, 202–207. doi:10.1016/j.jastp.2017.08.008

Albert, J. M., and Young, S. L. (2005). Multidimensional quasi-linear diffusion of radiation belt electrons. *Geophys. Res. Lett.* 32, L14110. doi:10.1029/2005GL023191

Birmingham, T. J., Northrop, T. G., Fälthammar, (1967). Charged particle diffusion by violation of the third adiabatic invariant. *Phys. Fluids* 10, 2389. Number 11. doi:10.1063/1.1762048

Brand, A., Allen, L., Altman, M., Hlava, M., and Scott, J. (2015). Beyond authorship: Attribution, contribution, collaboration, and credit. *Learn. Pub.* 28, 151–155. doi:10.1087/20150211

Fälthammar, C.-G. (1968), Radial diffusion by violation of the third adiabatic invariant, in *Earth's particles and fields*. B. M. McCormac (New York: Reinhold), 157

Fejer, B. G. (1993). F region plasma drifts over Arecibo: Solar cycle, seasonal, and magnetic activity effects. *J. Geophys. Res.* 98 (8), 13645–13652. doi:10.1029/93JA-00953

Lejosne, S., Fedrizzi, M., Maruyama, N., and Selesnick, R. S. (2021). Thermospheric neutral winds as the cause of drift shell distortion in Earth's inner radiation belt. *Front. Astron. Space Sci.* 8, 725800. doi:10.3389/fspas.2021.725800

Lejosne, S., and Albert, J. M. (2023). Drift phase resolved diffusive radiation belt model: 1. Theoretical framework. *Front. Astron. Space Sci.* 10, 1200485. doi:10.3389/fspas.2023.1200485

Lejosne, S., and Kollmann, P. (2020). Radiation belt radial diffusion at Earth and beyond. *Space Sci. Rev.* 216, 19. doi:10.1007/s11214-020-0642-6

O'Brien, T. P., Claudepierre, S. G., Guild, T. B., Fennell, J. F., Turner, D. L., Blake, J. B., et al. (2016). Inner zone and slot electron radial diffusion revisited. *Geophys. Res. Lett.* 43, 7301–7310. doi:10.1002/2016GL069749

Roederer, J. G. (1970). *Dynamics of geomagnetically trapped radiation*. Heidelberg: Springer Berlin. doi:10.1007/978-3-642-49300-3

Schulz, M., and Lanzerotti, L. J. (1974). *Particle diffusion in the radiation belts*. Berlin: Springer. doi:10.1007/978-3-642-65675-0

Selesnick, R. S. (2012). Atmospheric scattering and decay of inner radiation belt electrons. *J. Geophys. Res.* 117, A08218. doi:10.1029/2012JA017793

Tao, X., Albert, J. M., and Chan, A. A. (2009). Numerical modeling of multidimensional diffusion in the radiation belts using layer methods. *J. Geophys. Res.* 114, A02215. doi:10.1029/2008JA013826

Tao, X., Chan, A. A., Albert, J. M., and Miller, J. A. (2008). Stochastic modeling of multidimensional diffusion in the radiation belts. *J. Geophys. Res.* 113, A07212. doi:10.1029/2007JA012985

Tao, X., Zhang, L., Wang, C., Li, X., Albert, J. M., and Chan, A. A. (2016). An efficient and positivity-preserving layer method for modeling radiation belt diffusion processes. *J. Geophys. Res. Space Phys.* 121, 305–320. doi:10.1002/2015JA022064

Ukhorskiy, A., Sitnov, M., Mitchell, D., Takahashi, K., Lanzerotti, L. J., and Mauk, B. H. (2014). Rotationally driven 'zebra stripes' in Earth's inner radiation belt. *Nature* 507, 338–340. doi:10.1038/nature13046

Whipple, E. C. (1978). U, B, K) coordinates: A natural system for studying magnetospheric convection. *J. Geophys. Res.* 83 (A9), 4318–4326. doi:10.1029/JA083iA09p04318

Appendix

We explain how we derived the expressions for $\langle(\Delta r)^2\rangle$, $\langle(\Delta\varphi)^2\rangle$, and $\langle\Delta r\Delta\varphi\rangle$ (Eq. 11), in order to obtain the diffusion coefficients required to solve the drift-diffusion equation.
A first-order Taylor expansion for the expressions of the total variations in radial and azimuthal locations (Eq. 10) yields:

$$\begin{cases} \Delta r = \dfrac{r_o^3}{B_E R_E^3}\displaystyle\int_t^{t+\Delta t} w(u)\sin(\varphi_o+\Omega u)du \\ \Delta\varphi = \Omega\Delta t \\ \quad + \dfrac{3M}{\gamma_o q B_E R_E^3}\left(2-\dfrac{3MB_E R_E^3}{\gamma_o^2 E_o r_o^3}\right)\displaystyle\int_t^{t+\Delta t}\int_t^u w(x)\sin(\varphi_o+\Omega x)dxdu \\ \quad + \dfrac{r_o^2}{B_E R_E^3}\displaystyle\int_t^{t+\Delta t} w(u)\cos(\varphi_o+\Omega u)du \end{cases} \tag{A1}$$

where r_o, φ_o, γ_o are the values for the radial and azimuthal locations, and Lorentz factor, at time, t, respectively.
The expression for the ensemble average of the square of the total variation of the radial displacement is:

$$[(\Delta r)^2] = \frac{r_o^6}{B_E^2 R_E^6}\int_t^{t+\Delta t}\int_t^{t+\Delta t}[w(u)w(v)]\sin(\varphi_o+\Omega u)\sin(\varphi_o+\Omega v)dudv \tag{A2}$$

Since $\Omega\Delta t \ll 1$, the variation in phase is not significant, and Eq. A2 becomes

$$[(\Delta r)^2] = \frac{r_o^6\sin^2(\varphi_o)}{B_E^2 R_E^6}\int_t^{t+\Delta t}\int_t^{t+\Delta t}[w(u)w(v)]dudv \tag{A3}$$

Since the signal w is a piecewise constant function, we have that:

$$w(u) = w_i \text{ for } iT \le u < (i+1)T \tag{A4}$$

And by definition of the white noise sequence, $[w_i w_j] = W^2\delta_{ij}$, where δ_{ij} is the Kronecker delta. As a result, expressing the time interval, Δt, as $\Delta t = NT + k$, where N is an integer, and $0 < k < T$:

$$[(\Delta r)^2] = \frac{r_o^6 W^2\sin^2(\varphi_o)}{B_E^2 R_E^6}(NT^2+k^2) \cong \frac{r_o^6 W^2 T\sin^2(\varphi_o)}{B_E^2 R_E^6}\Delta t \tag{A5}$$

As a result:

$$\langle(\Delta r)^2\rangle = \frac{[(\Delta r)^2]}{\Delta t} = \frac{r_o^6 W^2 T}{B_E^2 R_E^6}\sin^2(\varphi_o) \tag{A6}$$

A similar approach allows for a computation of $[(\Delta\varphi)^2]$, and $[(\Delta r\Delta\varphi)^2]$ as first order functions of Δt, yielding analytical expressions for $\langle(\Delta\varphi)^2\rangle$, and $\langle\Delta r\Delta\varphi\rangle$. Alternatively, the total variation in phase, $\Delta\varphi$, can also be related the total variation in radial displacement, Δr, and the time variation, Δt, by considering a multivariate Taylor expansion for the expression of total energy conservation (e.g., Whipple, 1978):

$$\begin{aligned} &E_k(r_o+\Delta r, \varphi_o+\Delta\varphi, t+\Delta t) + qV(r_o+\Delta r, \varphi_o+\Delta\varphi, t+\Delta t) \\ &\quad = E_k(r_o, \varphi_o, t) + qV(r_o, \varphi_o, t) \end{aligned} \tag{A7}$$

where $E_k = E_o\left(\sqrt{1+2MB/E_o}-1\right)$ is the kinetic energy, with E_o the rest mass energy.
The formula provided Eq. A6 is not dependent on the energy of the particles considered, provided that the drift period is very long in comparison with the updating time, T. If we were to consider particles of higher energies, with a drift period smaller than the updating time, T, the magnitude of the radial diffusion coefficient would drop, in accordance with theoretical expectations. Indeed, with $\Delta t = k < T$, $N = 0$, and $[(\Delta r)^2]$ Eq. (A5) would become proportional to $W^2\Delta t^2 (< W^2 T\Delta t)$. In parallel, the ensemble average of the signal, $[w]$, would not be 0 anymore during Δt: this means that the effects of field fluctuations would be accounted for through the transport coefficients, $[\dot{\mathbb{L}}]$ and $[\dot{\varphi}]$ (Eq. 9).

Glossary

(α,β)	Euler potentials
$\boldsymbol{B}$	Magnetic field
B_E	Magnetic equatorial field at the Earth's surface
C	constant to model the corotation potential
D_{XY}	Diffusion coefficient with respect to the X and Y coordinates
$\boldsymbol{E}$	electric field
f,F	Distribution functions
γ	Lorentz factor
J	second adiabatic invariant
L^*	L-star, inversely proportional to the third adiabatic invariant
$\mathbb{L}$	double-struck L, or L-Euler
L	normalized equatorial radial distance
M	first adiabatic invariant
Ω_E	angular velocity of the Earth's rotation
$\Omega/2\pi$	unperturbed drift frequency
q	electric charge of a particle
r	radial location at the magnetic equator
R_E	Earth's equatorial radius
φ	Azimuthal location (i.e., magnetic local time, in radians)
τ_B	Bounce period
τ_D	Drift period
$t,\Delta t$	Time, small time interval
T	updating time for the sequence of outcomes w(t)
V	Electric potential
w	random variable
W	standard deviation of the random variable w
[ ]	Square brackets = expected value (average value over an ensemble of fluctuations) of the bracketed quantity
< >	Angle brackets = average change per unit time of the bracketed quantity ($= \frac{[]}{\Delta t}$)
$\propto$	Proportionality symbol